Experiments on rift zone evolution in unstable volcanic edifices

Thomas R. Walter [a,*], Valentin R. Troll [b]

[a] *University of Miami, MGG/RSMAS, 4600 Rickenbacker Causeway, Miami, FL 33149, USA*
[b] *Department of Geology, University of Dublin, Trinity College, Dublin 2, Ireland*

Abstract

Large ocean island volcanoes frequently develop productive rift zones located close to unstable flanks and sites of older major sector collapses. Flank deformation is often caused by slip along a décollement within or underneath the volcanic edifice. We studied how such a stressed volcanic flank may bias the rift zone development. The influence of basal lubrication and lateral flank creep on rift development and rift migration is still poorly constrained by field evidence; here our analog experiments provide new insights. We injected colored water into gelatin cones and found systematic orientations of hydro-fractures (dikes) propagating through the cones. At the base of the cone, diverse friction conditions were simulated. By variation of the basal creep conditions we modeled radial dike swarms, collinear rift zones and three-armed rift systems. It is illustrated that a single outward-creeping flank is sufficient to modify the entire rift architecture of a volcano. The experiments highlight the general unsteadiness of dike swarms and that the distribution and alteration of weak substratum may become a major player in shaping a volcano's architecture.
© 2003 Elsevier B.V. All rights reserved.

1. Introduction

Dikes are the common witnesses of magmas ascending in fracture-type pathways through the crust. Most volcanic eruptions start above feeder dikes, but only a small fraction of those dikes ever reaches the surface (Gudmundsson et al., 1999).

Driven by high magmatic pressure, the orientation of such a *propagating magma-filled fracture* strongly depends on the local stress pattern. The dike orientation is in general perpendicular to the minimum principal compressive stress, hence indicative of the stress field within a volcano (cf. Anderson, 1937). If a temporarily steady stress system dominates a volcanic edifice, dikes may group to form swarms and rift zones. These are principally vertical structures formed by hundreds or thousands of parallel-striking magma paths (Fiske and Jackson, 1972; Walker, 1999). Such zones may contribute to the endogenic growth

* Corresponding author; formerly at Dept. of Volcanology, GEOMAR, Kiel, Germany.
E-mail addresses: twalter@rsmas.miami.edu (T.R. Walter), trollv@tcd.ie (V.R. Troll).
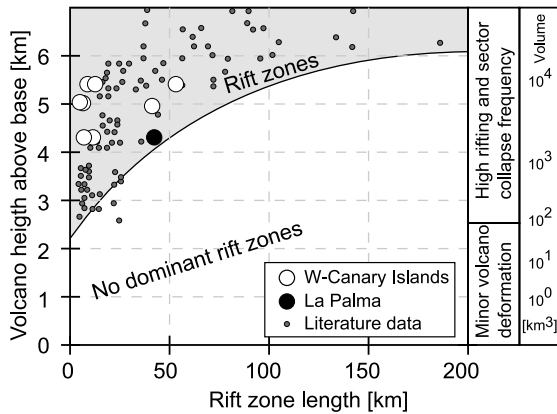
Fig. 1. Rift zone lengths (*x*-axis) as a function of oceanic volcano height above the base (*y*-axis) and estimated volcano volume. Rift zones commonly form and elongate on higher volcanoes (modified after Mitchell, 2001; includes data from Vogt and Smoot, 1984).

of volcanic edifices by up to 30% or more (Annen et al., 2001; Walter and Schmincke, 2002).

The significance of rifting seems to increase with size of the volcano. Rift zones form in particular within larger volcanic edifices, indicative of the importance of gravitational stresses (Vogt and Smoot, 1984; Walker, 1987, 1992). Fig. 1 summarizes morphological data sets of seamounts and

volcanic islands, showing the length of rift zones to increase rapidly at volcanoes taller than 3 km (Mitchell, 2001).

A change to a volcano's stress field will also alter the direction of dyke intrusion and modify the position of an entire rift zone if the stress change is sufficient enough. The structural axis of a rift zone is thus not a permanent feature and can migrate laterally, as e.g. proposed for some Hawaiian dyke swarms (Swanson et al., 1976). In experiments, Fiske and Jackson (1972) showed the importance of the volcano load and stress distribution for the formation of rift zones on volcanoes. Following their results, the topography of a volcano directs the dike paths where rifting is parallel to e.g. a topographic ridge (Fig. 2). The gelatin analog models of Fiske and Jackson were recalculated by Dieterich (1988), who found that volcanic flanks must dilate laterally to overcome a plumbing effect. The presence of weak substrata (e.g. deformable ocean sediments and/or olivine cumulates) provides, potentially widespread décollement zones at a volcano's base (Nakamura, 1980; Clague and Denlinger, 1994; Delaney et al., 1998; Borgia et al., 2000). Similarly, viscous substrate upon which volcanoes may be built can cause volcanoes to spread laterally,
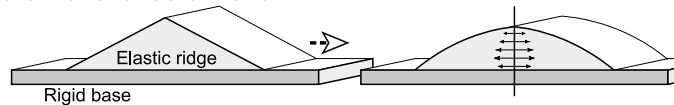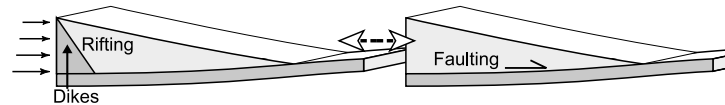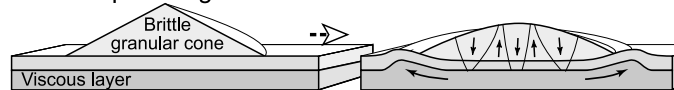
Fig. 2. Three major types of gravity-driven volcano deformation. (A) Gravitational deformation of elastic ridge produces horizontal expansion along the axis of symmetry; i.e. persistent rifting is gravity-driven (Fiske and Jackson, 1972). (B) Forceful intrusions in rift zone accumulate the driving stress for lateral slide, extension drives rifting persistence (feedback mechanism after finite element modeling of Dieterich, 1988), e.g. ocean sediments form a weak substratum and facilitate décollement of volcano flanks. (C) Volcano spreading describes a specific type of flexure and basal deformability. Analog models above a thin viscous layer result in lateral expansion, formation of a circumferential bulge, horst and graben structures on the edifice flanks, and apex subsidence (after Merle and Borgia, 1996).
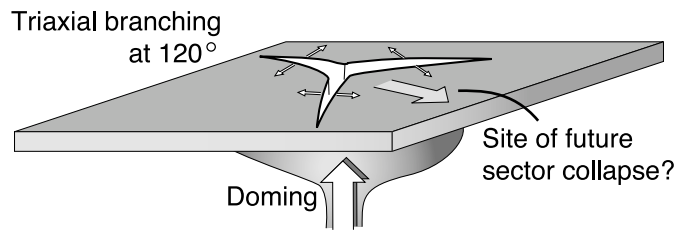
Fig. 3. Least-effort model as previously proposed for the origin of triaxial rift geometries on the Canary Islands (see text for details).

purely driven by their own weight (Borgia, 1994; Merle and Borgia, 1996; Borgia et al., 2000; Walter, 2003). The southern Kilauea flank expands on such a basal sliding surface, opening the space for dikes of the Kilauea rift system (Dieterich, 1988). Volcanic spreading is a process that is meanwhile proposed to control the rifting procedure and structural evolution of many large volcanoes (e.g. Borgia et al., 2000; Walter, 2003).

Despite these advances in understanding volcano deformation, it remains unclear in what way particular rift zones develop. Endogenously driven mechanisms are thought to play a major role in establishing axial volcano architectures. For instance, the concept of formation of regular triaxial rift zones on the Canary Islands is adapted from plate tectonics, where triple-armed junctions are believed to form in response to vertical upward loading (McFarlane and Ridley, 1968; Luongo et al., 1991; Carracedo, 1994, 1996). In view of that, regular triple-armed rift zones on volcanoes result from the least-effort fracturing mechanism of the brittle crust (Carracedo, 1996). This least-effort model (Fig. 3) is considered to explain (a) the aligned concentration of eruptive sites on the western Canaries (Tenerife, El Hierro and La Palma), (b) the longevity and direction of rift zones, and (c) the genesis of volcano sector collapses located in-between two ∼ 120° rift zones (Carracedo, 1994, 1996). In contrast, studies that focused on volcanic doming revealed radial and concentric dike swarms exclusively (e.g. Komuro et al., 1984; Marti et al., 1994; Walker, 1999; Walter and Troll, 2001; Troll et al., 2002). Three-armed rift zones have, in fact, not been experimentally reproduced previously, suggesting other mechanisms to control

this type of rift formation, leaving the least-effort hypothesis open for rigorous experimental tests. 'On particular islands (e.g. Tenerife or Hawaii), a number of triaxial rift zones developed simultaneously. The centers of those rift systems are located in close proximity to each other (often < 20 km only). In the sense of upper mantle (high) viscous relaxation behavior and flexure wavelengths of the crust (e.g. Watts, 2001), and by knowing about the closeness of those rift zones, it seems illusive that deep mantle forces and crustal doming could be responsible for all those triaxial rift zones on one island.'

Therefore, the question arises whether rifting is a consequence of flank deformation, or rifting causes a flank to deform. High magmatic and hydrothermal pressures that accompany dike intrusions are thought to force these volcanoes to expand laterally, thus pushing the flanks of a volcano to creep seaward (McGuire et al., 1990; Iverson, 1995; Elsworth and Voight, 1995, 1996). The locations of lateral collapses and sector slips of volcanic flanks are frequently enclosed by two rift zones of a triaxial system. For intrusive flank push and sector slip along low-inclined detachment surfaces, the basal shear resistance and the angle of internal friction must be very low, with weak substrata resembling lubrication planes (cf. Iverson, 1995). It remains unclear, however, at what stage of volcano evolution rift zones are initiated, and how proceeding sector slip modifies a given rift pattern. Since dike direction and volcano flank instability (i.e. sector slip) are functions of a volcano's gravitational load, these two processes are interlinked, i.e. changing one parameter would ultimately alter the other. Our study addresses the questions how a volcano

stress field affects the rifting directions and how a given rift pattern is modified by local mechanical inhomogeneity and substrata detachment.

2. Experimental procedure

We dissolved powdered gelatin in 60°C water at a concentration ∼2.5 wt%. The solution was filled into cone-shaped molds and then refrigerated for 12 h. We used a range of diverse cone-shaped molds to simulate various 'volcano' geometries. The base of the molds was between 50 and 400 mm in radius, heights were 50–200 mm, with a flank steepness of 45° to about 25°. The hardened gelatin 'volcanoes' were placed on a PVC plate. Small holes were drilled into the plate to accomplish injection of a liquid (the magma) through a syringe-pipe system. As a consequence of gravitational deformation on removal of the upside-down turned mold, the cone height shrank and the plane perimeter increased. Following injection of colored water into the cones from underneath, the propagation and direction of fluid-filled fractures was recorded.

2.1. Materials used

Gelatin is characterized by linear viscoelastic behavior at small deformations (Richards and Mark, 1966), with a shear modulus G depending strongly on velocity (Bot et al., 1996). The rheological behavior of gelatin was examined in creep tests, indicating a short-term 'Voigt body deformation' (elastic behavior) and 'Maxwell body

flow' for long time duration (Richards and Mark, 1966). This means that the stress–strain curve – whose slope is defined as the 'Young's modulus' – depends on the rate of strain. A consequence is the brittle behavior at high strain rates, being controlled herein by the injection rates. The strength of gelatin depends upon the concentration and intrinsic strength of the gelatin used (here: bloom strength 170 g). Other factors affecting the rigidity of gelatin include its temperature and the thermal history, which was held constant throughout all experiments. The physical parameters of natural rocks were not to scale in our experiments and the results are considered to be qualitative. To test the influence of various gelatin strengths, we changed the concentration of the gelatin powder and repeated the experiments, generally reproducing the same arrangements of fractures (see below).

The solute gelatin gel has a Poisson ratio of nearly 0.5, the condition in gelatin thus being approximately hydrostatic. If fracturing occurs, the finite yield strength is exceeded. On injection, vertical hydraulic fractures form when the injection pressure is greater than the sum of the gelatin's yield strength and the minimum compressive stress that acts in the horizontal plane. The injected liquid caused cracks propagating mainly laterally under low injection pressure (∼2 ml/min). For higher injection pressures, the vertical propagation axis amplified. In profile, for higher pressures or if the liquid was more viscous, the thickness of the cracks increased. This elasticity effect may likewise be found on volcanoes, which deform elastically before fracturing occurs and dikes
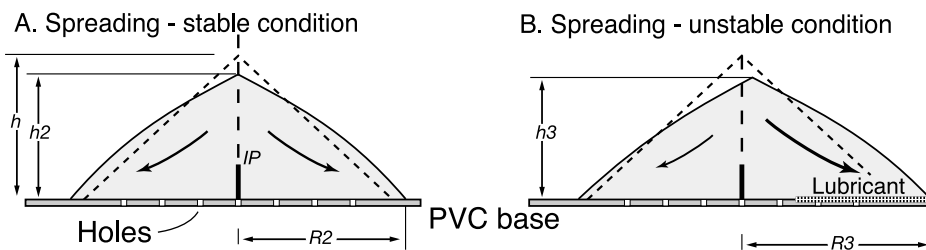
Fig. 4. Geometry of experimental cones in stable situation (A) and unstable situation (B). Due to gravity, the cones spread outward, partially sliding on a basal lubricant. In the unstable situation, only one flank was lubricated. IP, injection point (10 mm above base), basal radii $R_3 > R_2 > R_1$; cone height $h > h_2 > h_3$. Through small holes drilled in the basal plate, injection was possible at various positions.
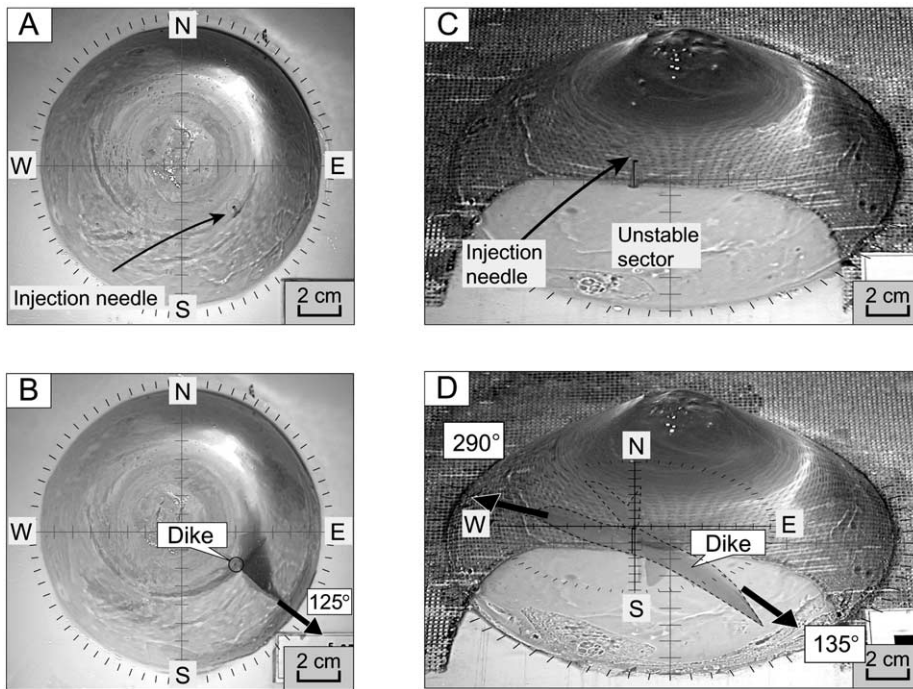
Fig. 5. Photographs of experiments before (panels A and C) and after injection (panels B and D). (A) Plan view of stable situation, forming (B) a radial dike oriented 125° azimuth on injection. (C) Oblique view of unstable situation with injection into the interface creeping/non-creeping sector and a slight southwestward eccentricity of the lubricated base. (D) Produced fractures to southeast (135°) and northwest (290°).

propagate, where the dike thickness generally decreases with lower magma viscosity and magmatic pressure. This is in accordance with magmatic pressure exceeding the tensile strength of the volcanic rock plus σ_3 acting in a horizontal plane, as suggested for Hawaiian volcanoes and by numerical modeling (e.g. Pollard et al., 1983; Ida, 1999).

2.2. Data analysis

First, we studied cone deformation with a homogeneous basal friction. In a second setup, we placed the gelatin cones onto a PVC plate that contained a low-friction sector to simulate the effect of total or partial flank creeping. These two setups are categorized into a *stable situation* and an *unstable situation*. In the stable-situation experiments, a soap-based lubricant greased the gelatin-cone base, so that the entire interface cone/ground represented a low-friction surface. In these experiments, the gravitational stress field of the cone caused uniform outward spreading of the flanks (Fig. 4).

In the unstable-situation experiments, a different PVC plate was roughened, except for one segment, allowing a defined sector of the cone to glide outward preferentially. We consider this unstable situation as an analog to a volcano stress field influenced by a flank that slides on a basal or volcano-internal subhorizontal detachment surface. The size of this décollement and the sliding direction were varied in different experimental setups. The propagation and orientation of the fractures were measured and recorded (Fig. 5). The experiments were divided into groups, defined by the locality of the injection points beneath the cones, and the size and the eccentricity of the creeping sector. Dyke trends are reported as imagined compass directions (N–S–E–W), on the basis of which standard tools of statistical azimuth analysis in stereographic projections were used (see Fig. 5).

To diminish side effects and pre-experimental strain of the gelatin by e.g. insertion of the needle from below, upside-down turning of the molds and slightly varying material properties, the experiments were evaluated statistically on the basis of more than 300 experimental runs. The large number of experiments allowed evaluation of mean dike directions for a specific geometrical situation. We did not study the details of multiple injections into a sole gelatin edifice, since gelatin rupture is an irreversible process and the previous fracture paths would act as traction free surfaces and generally modified the stress field. A further (e.g. regional) tectonic influence was also not simulated.

3. Experimental results

3.1. Stable situation (homogeneous basal shear resistance)

We injected the liquid into the cone's flanks or into the axis of symmetry of the cone. If injected into the flanks of the cone, the fractures propagated towards the nearest free surface of the cone, i.e. radially away from the cone's center (Fig. 6). When injected very close ($< \sim 2$ cm of 10-cm-wide cones) to the axis of symmetry, the azimuth of the fractures seemed to be of various orientations. On further injection and advanced outward-directed fracture propagation, the fractures curved into a radial orientation. A radial fracture pattern in an elastic cone that is placed on a homogeneous base can be explained by gravity-driven deformation that causes circumferential flank extension all around the cone, with radial maximum principal-stress directions in plan view. The sole influence of the cone load on crack propagation is thus principally consistent with experimental findings by McGuire and Pullen (1989) and Merle and Borgia (1996).

3.2. Unstable situation (inhomogeneous basal shear resistance)

Gelatin cones were partially placed on a high-friction surface and partially above a slippery 'dé-
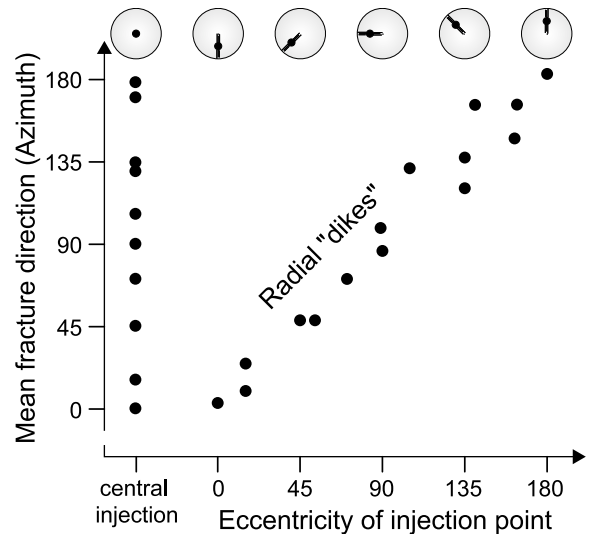
Fig. 6. Stable situation: Relation of mean hydro-fracture propagation direction to the eccentricity of the injection point (measured in azimuth). Situated on a uniform substratum, the flanks of the gelatin cone deformed by gravity-driven extension only. Central injection beneath the apex of a regular cone generates randomly directed fractures. Injection into the cone flanks produces fractures oriented radially, i.e. away from the edifice center.

collement' sector, imitating a volcano that deforms above a locally restricted layer of mechanical weakness (Fig. 5C). The resulting stress field qualitatively imitates a volcano that deforms locally above a restricted weak layer. We repeated these experiments and systematically varied site and size of the unstable sector and the point of injection. First, we studied the importance of the flank-creep direction. We placed the gelatin cone in such a way that its southern flank glided southward (no E–W eccentricity). On injection, fractures formed that were similarly oriented on the east and west sector of the volcano (Fig. 7A–C, panels 1). In other words, the north–south axis formed the axis of symmetry in plan view. If creep direction of the sector was changed towards a slightly east or west eccentricity, uneven fractures formed on either side of the cone (Fig. 7A, 2–3; Fig. 7B, 2–4; Fig. 7C, 3–4). For instance, gliding of the southern sector down to the southwest enforced the principal and longest dikes to form into the southeastern sector of the cone. On the oppo-
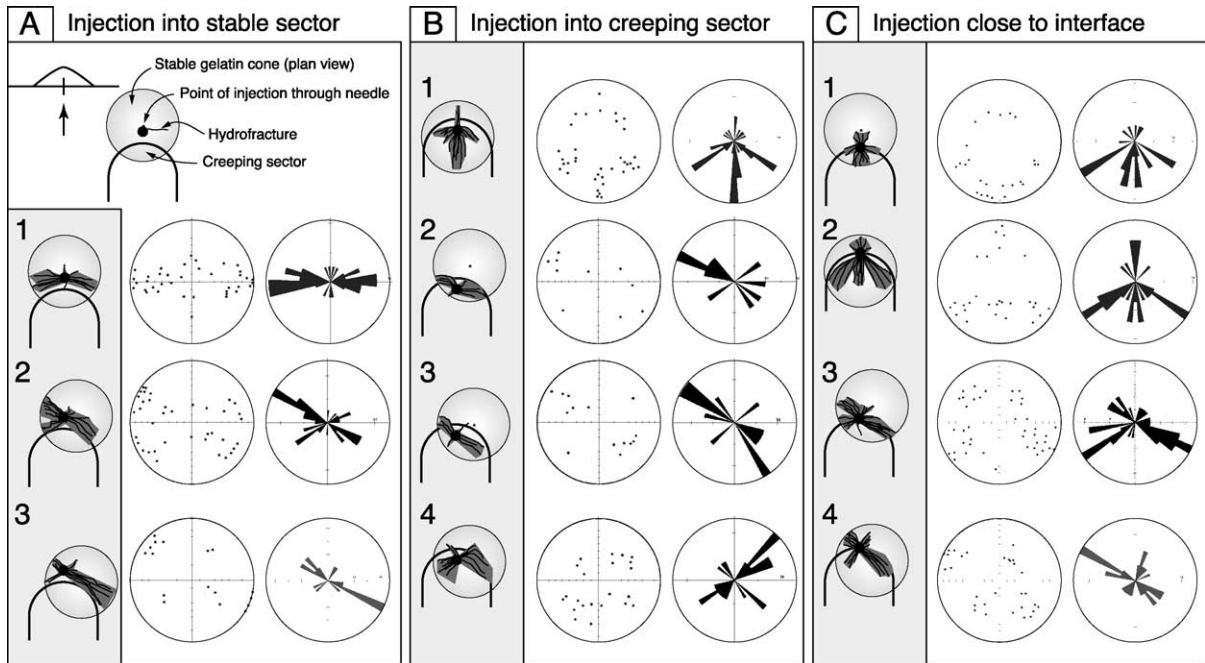
Fig. 7. Summarized arrangement of hydro-fractures propagating in locally destabilized edifices relative to injection point and eccentricity of a creeping sector. (A) Injection into stable sector. (B) Injection into creeping sector. (C) Injection close to the interface stable/unstable sector. Stereoplots illustrate the statistic orientation of fractures: each black dot in pole plots refers to the distal locality of an experimental fracture, measured in azimuth and distance from the point of injection. In frequency–azimuth (rose) diagrams (polar lines, sector size = 8°), the length of each rose sector is proportional to the frequency of orientation that lies within that sector.

site side of the unstable sector strike-slip faulting may form.

The location of the injection point relative to the cone and its unstable sector has a further influence on the above relations:

(a) Injection into the stable sector of a cone caused dikes that strike mainly tangentially around the creeping sector (Fig. 7A). Here, dike paths were mainly oriented east–west. With further outward propagation, the fractures turned perpendicularly to the cone's perimeter (radial). The tendency of adopting a volcano-radial direction increased with distance to the lubricated part and to the volcano midpoint, i.e. the greater the distance of injection from the unstable sector, the larger the number of radial trends.

(b) Injection into the creeping sector of the cone produced orientations markedly different from those described above (Fig. 7B). When the unstable sector was centered with southward sector-

creep direction, curved fractures formed in the north–south direction, and tangentially to the creeping sector (i.e. east–west). These dike directions varied with increasing creep influence: when 10% of the cone creeps southward, the main dike direction was east–west (i.e. tangential), with radial influence acting only very close to the free flank. When more than ∼20% of the cone's base was on a weak substratum, the liquid intruded mainly into two or four directions: two axes with strong tangential trend curving around the creeping/non-creeping interface. Frequently, two further axes developed perpendicularly to the former into a north–south direction (Fig. 7B). All those main axes were restricted to the southern unstable part of the cone. The main dike directions also migrated with varying creep direction of the unstable sector. Slight eccentricity of the basal lubrication plane to the southwest resulted in a major southeast–northwest fracture

direction (in analogy, eccentricity to the southeast resulted in major southwest–northeast fractures). In experiments when a very large part or the entire cone was creeping (simulating e.g. downslope creep), dikes were concentric only very close to the interface of a stable remnant. In the main part of the cone, dikes arranged in a more diffuse fashion in the creep direction. This seems to be a consequence of basal friction, i.e. compression of the cone's base in the creep direction.

(c) Injection directly above the interface of the creeping sector to the stable cones frequently caused three major dike directions of variable pronunciation (Fig. 7C). Both direction and pronunciation of these axes were dependent on the direction of sector creep and the point of injection. Three main trends were commonly defined: two sector-tangential directions, plus a third trend into the stable cone. The location of the third, more diffuse trend was a function of the position and pronunciation of the two tangential dikes. When a cone was unstable e.g. in the SW flank, the main tangential trend was SE, the secondary tangential rift axis was propagating to the west. The third diffuse swarm then grew into the stable area to the NE–NW (Fig. 7C, panel 3). The two principal directions (west and southeast) were tangential to the interface stable/unstable cone, again outlining the approximate size of the lubricated sector beneath.

3.3. How many rift axes?

In the stable situation (Fig. 8A), 60% of injections initiated one fracture, statistically the orientation was radial. The unstable situation, in contrast, resulted regularly in multiple major orientations (Fig. 8B): Injection into the stable sector caused four axes in 20% of the experiments, but mostly only a single axis. Injection into the creeping sector produced a single rift zone in >55% of the experiments, and two, three and four axes in <45% of experimental runs. When injected close to the interface stable/unstable sector, three directions developed in ca. 70% of the experimental runs. Two of the axes were well pronounced as curved tangents to the margin of the creeping sector and a third, less strongly defined arm was directed into the stable part of the volcano (Fig. 8D).

The third rift commonly formed subsequently to the development of the tangential arms and formed only when the tangential arms were significantly curved. Consequently, the transition from single rift to two sector-tangential rift zones or even a triaxial architecture was controlled by
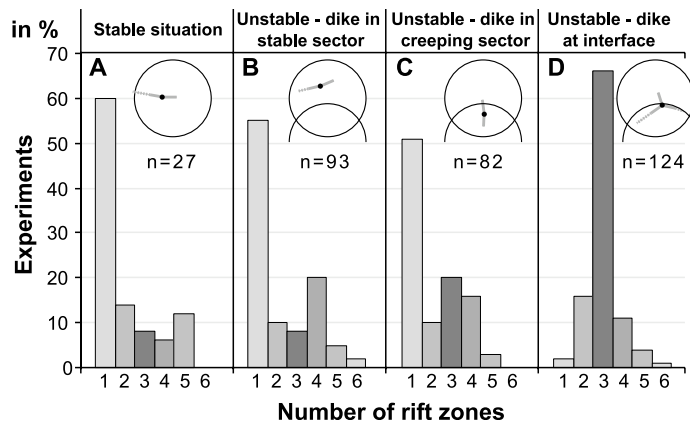
Fig. 8. Number of rift zones as a function of total number of experiments (in %). (A) Stable experiments caused on single injection mainly two radial fractures. (B) Unstable situation resulted – when injected into the stable sector – in mainly two or four emergent directions. The angle between fracture azimuths was more than 100°. (C) Injection into the creeping sector resulted in most of the cases in single trends, three axes in 20% of experiments. (D) Injection into the interface stable/unstable sector produced in approximately 65% triaxial rift zones. When a flank starts to creep, the result will be that the number of rift zones changes. See text for details.

the presence of a creeping sector and intrusive locality. The third arm is thus likely to develop due to local tension resulting from the compression induced by dilation at the two main tangential rift zones – a causality that was obtained in 65% of our experiments.

4. Discussion

Gelatin-cone models show how the stress field and propagating hydro-fractures reconfigure due to the influence of a creeping sector. By injecting colored water into these gelatin cones we studied the fracture paths and found a systematic pattern that reflects sector creep conditions. Since the cones are breached on injection by (a) radial fractures when the basal friction is homogeneous, but form (b) discrete rift zones when a cone's sector was partially located on a basal lubricant, we assume volcanoes and their intrusive sheets to follow similar principles, reflecting detachment of edifice sectors above weak (substratum) layers. Inferring volcanoes behave, in principle, similarly to our experiments, our observations imply that special circumstances are needed to create a triaxial rift system, as shown for the experiments with varying injection positions. A key incident is that magma migration is permitted close to the interface between the stable and unstable part of an edifice. This may also mean that a lateral magma migration eases triaxial rift zone formation. Transition from a single rift towards strongly curved or two separated sector-tangential rifts may promote a third rift. The triaxial architecture thus appears characteristic for a volcano that is centrally supplied and experiences increasing instability of a sector. The rift zone that is less pronounced is commonly located in the stable part of the volcano, while the stronger rifts are tangential to the creeping sector.

In nature, rift zones occur on most oceanic islands and are characterized by dense dike swarms with a concentration of eruptive centers above. Accumulating dikes form coherent intrusion complexes, making up the structural framework of large ocean island volcanoes, such as those of the Hawaiian and the Canary archipelagoes (e.g.

Walker, 1992; Carracedo, 1996). Walker (1992) termed rift zones as being 'possibly an invariant component' controlling the evolution of ocean island volcanoes. For the Hawaiian volcanoes, Walker (1992) described that two collinear rift zones may become non-collinear when asymmetric growth occurs, e.g. due to buttressing effects. This means that, even without basal lubrication, dikes may arrange into two rift zones and cause extension on the opposite side of the nucleus to form the potential site of a third rift arm. Likewise, buttressing barriers may influence size and direction of volcano sector creep and e.g. hamper the development of a third rift zone if reinforced by an outsized hinterland. Our models show that directions of hydro-fractures reconfigure due to a laterally creeping flank. The reasons of flank creep on lubricants can be various since volcanic materials have an extremely wide range of mechanically different properties. Basic average compressive strength (and *shear strength*) values may vary from 100 to 300 MPa (20–60 MPa shear strength) for basalt, from 35 to 50 MPa (10–30 MPa) for volcanic breccia and welded tuff, ∼10 MPa (∼5 MPa) for fine-grained tuff, to less than 5 MPa (<3 MPa) for weathered rocks such as paleosoil (e.g. Attewell and Farmer, 1976; Aversa and Evangelista, 1998; Watters et al., 2000). Also of significance is porosity and pore water, which can easily reduce the unconfined compressive strength by up to 60%. Hydrothermal alteration may decrease initially strong materials by two orders of strength magnitude and drastically decrease the internal friction coefficient (Watters et al., 2000). As a consequence, lubrication planes may form in all levels within volcano successions and may develop relatively late in a volcano's evolution.

On each of the younger (western) Canary Islands, rift zones underlie the aligned vent locations characterized by parallel dike orientations. On Tenerife and El Hierro three major rift zones are arranged in a triaxial configuration, systematically enclosing ∼100° to ∼140° angles in between (Carracedo, 1994; Walter, 2003). The azimuths of these main rift zones and the directions of giant landslides are clearly related. Elsworth and Voight (1996) described extensional stresses in volcanic edifices that are interconnected to

phases of intense intrusive/eruptive activity. These stresses may reach the rupture threshold and trigger massive landslides. More than 50% of the total subaerial volumes of the western Canary Islands collapsed laterally into the sea or were eroded during the past million years (Carracedo et al., 1999a,b).

La Palma, the westernmost Canary Island, shows an evolutionary and structural dichotomy (Fig. 9): an old circular shield in the north (Garafia and Taburiente volcanoes), from which later the 25-km-long Cumbre Nueva/Cumbre Vieja rift zone extended subaerially to the south (the *Cumbre Ridge*). The northern, old shield is composed of a Pliocene submarine and plutonic core that is uplifted by over 1 km and tilted to the southwest (Staudigel and Schmincke, 1984; Carracedo et al., 2001a). Above an erosional unconformity, this succession is covered by subaerial lavas. Repeated gravitational collapses in the southern and southwestern sector significantly influenced the successive volcanic evolution, as is best visible by fissure (re-)configurations (Carracedo et al., 2001a).

Northern La Palma's shield volcano was structurally controlled by radial fissures (Ancochea et al., 1994), forming a deep-reaching radial dike swarm for about 1 Ma (Day et al., 1999; Carracedo et al., 2001a,b; Guillou et al., 2001). At about 0.8 Ma, this radial configuration was progressively superseded by rift zones, one subordinate rift to the NW, one to the NE, while first signals of the increasingly productive Cumbre Ridge developed to the south (Ancochea et al., 1994; Carracedo et al., 2001a). If volcanism did not drift to the south, Carracedo et al. (2001a) hypothesized, all those rift zones would have emerged and produced volcanic ridges. We assume, however, that this radial persistence of Taburiente volcano ceased due to a type-scenario of the interplay of constructive and destructive episodes. The sector that was enclosed by the northwest rift and the intensifying south rift collapsed southwestwards into the sea at ∼0.56 Ma (Guillou et al., 2001; Carracedo et al., 2001a,b). Based on borehole and age data, Carracedo et al. (1999b) interpreted the contact between the much older seamount series and the post-collapse Bejenado volcano (0.55 Ma) as the interface of the collapse boundary. Increased productivity of the southern rift arm, between 0.8 and < 0.56 Ma, caused a morphological ridge to migrate southward. We conjecture this southward rift migration to be a consequence of the unstable and creeping southwestern volcano sector that eventually collapsed at 0.56 Ma.

In our gelatin experiments, a creeping flank of a radial cone also caused two main sector-tangential fracture trends. If the unstable sector was eccentric, e.g. to the southwest, one of these experimental rifts developed more strongly than the other. In these experiments, hydro-fractures propagated sector-tangentially to the west and principally to the south. By analogy, the pronounced Cumbre dike swarm on La Palma may reflect the response to southwestward sector creep. The dikes grouped to form tangential rifts, replacing an initially radial dike swarm, with volcanic productivity subsequently migrating southward. On the basis of our experimental observations, we infer that the recently active La Palma south rift may have been initiated during early stages of flank instability, consistent with the suggestion by Carracedo et al. (2001a) that the structures that control rift zones on La Palma have formed early in the volcano's history. The sequence above the southwestward-tilted seamount was then detached in the southwest. Analogous to the sector-tangential fracture direction in our unstable gelatin experiments, the lasting and dominant tangential Cumbre rift zones formed (Fig. 9). Although other mechanisms may also have played a role in the structural evolution of La Palma, our experimental observations suggest a causal link between flank instability and migration of the volcanic activity to the south of La Palma. Once, however, a cone was established on the southern flank of the northern shield, the amalgamated edifice may have acted similarly to a volcanic ridge (cf. Fiske and Jackson, 1972), additionally strengthening north–south rifting due to buttressing effects (Carracedo et al., 2001a; Walter, 2003).

The southern flank of Hawaii Big Island is the type-example where flank creep over weak décollement has been proposed. For Kilauea, sliding may occur seismically or aseismically during or in between major intrusive events (e.g. Dvorak,
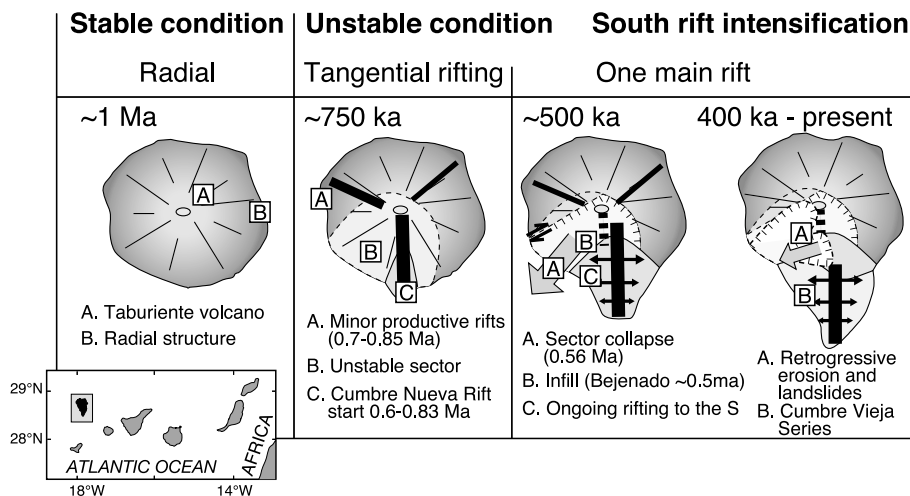
Fig. 9. Structural evolution of La Palma (includes data from Ancochea et al., 1994; Carracedo et al., 1999b, 2001a,b; Guillou et al., 2001). The position and direction of the creeping flank favored extension in an east–west direction in the southern flank, and thus the formation of a north–south rift zone. Once formed, the main south rift stabilized itself by alternating constructive and destructive processes. See text for explanation.

1994; Ryan, 1988; Delaney et al., 1993; Cervelli et al., 2002). The loci and extent of the individual thin décollement planes are still in question, however. Most likely, the basal Kilauea fault is almost horizontal and roots at depth at the rift's base. The thickness of the proposed décollement is very small (1%) compared to the volcano height (Borgia, 1994). Sliding along this décollement plane is believed to occur largely in aseismic fashion, interpreted to be an effect of large Coulomb stress changes along the fault zone (Tilling and Dvorak, 1993; Troise, 2001). The site of detachment well fits the location of weak materials close to the interface of the volcanic base to the ocean crust at a depth of ∼9 km (Clague and Denlinger, 1994; Delaney et al., 1998). This lubricating interface extends laterally along ancestral landslide debris and pelagic sediments (Moore et al., 1989). The seaward-directed flank motion is interpreted to be driven by the mass of the volcano and by 'magma push' (Denlinger and Okubo, 1995; Owen et al., 1995; Delaney et al., 1998). Of interest is the asymmetric seismicity across the Kilauea rifts, being focused at the seaside and practically absent north of the rift (Ryan, 1988; Tilling and Dvorak, 1993). Theoretical studies of dike pressure, however, predict a symmetric pattern of

Coulomb stress on either side of the rift (Rubin and Pollard, 1987). This discrepancy could be the result of a buttressing barrier (Mauna Loa) at the northern onshore side, or an effect of the concave curvature of the rift (cf. Ryan, 1988; Troise, 2001). Once established, gravitational spreading of topographic ridges (cf. Fiske and Jackson, 1972) and a density increase nearer to the dike complex (cf. Walker, 1992) contribute to lasting activity of rift zones. The evolution from flank creep to rift zone forming dikes is hence likely to represent the components of a positive feedback pattern. Weak substratum and gravity-driven creep of volcano flanks are thus suggested to control near-surface rifting of volcanic edifices and therefore the structural framework of volcanoes. In this context, formation and configuration of triaxial rift zones is very likely to be a response to near-surface volcano deformation such as volcano-flank creep, rather than a simple function of vertical upward loading as previously assumed for volcanic rifts on ocean island volcanoes.

5. Summary and conclusions

In gelatin experiments we varied the configura-
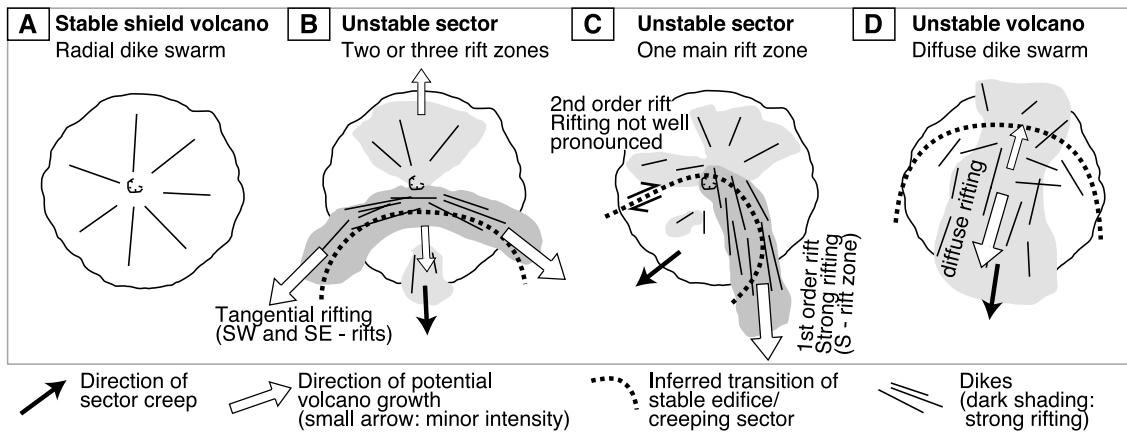
Fig. 10. The persistence and direction of three main rift zones varied systematically in size, eccentricity and creep direction of the unstable sector. (A) Radial volcano; spreading with homogeneous basal shear resistance. If a sector of a radial volcano starts to creep laterally, we can expect one of three principal structural configurations. (B) Two main rift zones form, possibly promoting a third rift on the opposite side. (C) Example of an eccentrically creeping flank that is bounded by right-lateral faulting (west flank) and strong expansion that facilitates rifting (here: south rift). Case C illustrates the projected structural development of a dominant tangential rift as seen on e.g. La Palma, Canary Islands. (D) A diffuse dike swarm is encouraged in the sliding direction if an edifice creeps (almost) entirely.

tion of analog cones (from stable to unstable) and then produced dikes whose orientations help to understand the stress field. Different conditions of basal friction were used in various experimental setups.

Situated on a uniform substratum, the flanks of the gelatin cone deformed by gravity-driven extension. The orientation of the fractures was perpendicular to the minimum principal compressive stress, resulting in a radial dike swarm. In a further setup, we reduced the basal shear resistance in one sector, to simulate the stress field close to a locally creeping flank. In these experiments, the dike azimuth diverged significantly when injected into (a) the non-creeping part of the cone, (b) the creeping sector, or (c) the stable/unstable interface. Case a produced radial fractures when the injection point is far enough from the unstable sector. Case b produced mainly fractures that reflect strong circumferential expansion of the creeping sector. In case c three main fracture directions formed, two of which were tangential to the stable/unstable interface and a third, diffuse one propagated into the stable part of the cone, reminiscent of triaxial rift zones on many ocean island volcanoes. The significance and direction of the three rift zones varied systematically with size,

eccentricity and creep direction of the unstable sector. Three main types of rift zone configurations may consequently develop from an initially radial volcanic cone (Fig. 10). Slight eccentricity of the creeping sector focuses dike intrusion along two curved axes tangential to the stable/unstable interface. In contrast, strong eccentricity resulted in only one main tangential rift, while other rifts remain poorly developed or strike-slip faults build up. With initiation of a creeping sector, an initially radial-structured volcano is therefore likely to reconfigure and produce rift zones that form one, two, or three axes. These results indicate that the formation of many triaxial rift zones is likely to be a response to near-surface volcano deformation. Therefore, flank creep may be a prime criterion for the initiation of this type of rift system.

References

Anderson, E.M., 1937. Cone sheets and ring dykes; the dynamical explanation. Bull. Volcanol. 1, 35–40.

Ancochea, E., Hernan, F., Candrero, A., Cantagrel, J.M., Fuster, J.M., Ibarrola, E., Coello, J., 1994. Constructive and destructive episodes in the building of a young oceanic island, La Palma, Canary Islands, and genesis of the caldera de Taburiente. J. Volcanol. Geotherm. Res. 60, 243–262.

Annen, C., Lénat, J.-F., Provost, A., 2001. The long-term growth of volcanic edifices: numerical modelling of the role of dyke intrusion and lava flow emplacements. J. Volcanol. Geotherm. Res. 105, 263–289.

Attewell, P.B., Farmer, I.W., 1976. Principles of Engineering Geology. Chapman and Hall, London, 1045 pp.

Aversa, S., Evangelista, A., 1998. The mechanical bahaviour of a pyroclastic rock: yield strength and 'destructuration' effects. Rock Mech. Rock Eng. 31, 25–42.

Borgia, A., 1994. Dynamic basis of volcanic spreading. J. Geophys. Res. 99, 17791–17804.

Borgia, A., Delaney, P., Denlinger, R.P., 2000. Spreading volcanoes. Annu. Rev. Earth Planet. Sci. 28, 539–570.

Bot, A., Groot, R.D., Agterof, W.G.M., 1996. Non-linear elasticity and rupture of gelatin gels. In: Phillips, G.O., Williams, P.A., Wedlock, D.J. (Eds.), Gums and Stabilisers for the Food Industry 8. IRL Press, Oxford, pp. 117–126.

Carracedo, J.C., 1994. The Canary Islands; an example of structural control on the growth of large oceanic-island volcanoes. J. Volcanol. Geotherm. Res. 60, 225–241.

Carracedo, J.C., 1996. A simple model for the genesis of large gravitational landslide hazards in the Canary Islands. In: McGuire, W.J., Jones, A.P., Neuberg, J. (Eds.), Volcano Instability on the Earth and Other Planets. Geol. Soc. London 110, 125–135.

Carracedo, J.C., Day, S., Guillou, H., Torrado, F.J.P., 1999a. Giant Quaternary landslides in the evolution of La Palma and El Hierro, Canary Islands. J. Volcanol. Geotherm. Res. 94, 169–190.

Carracedo, J.C., Day, S., Guillou, H., Gravestock, P., 1999b. The later stages of the volcanic and structural evolution of La Palma, Canary Islands: The Cumbre Nueva giant collapse and the Cumbre Vieja volcano. Geol. Soc. Am. Bull. 111, 755–768.

Carracedo, J.C., Badiola, E.R., de la Nuez, J., Perez Torrado, F.J., 2001a. Geology and volcanology of La Palma and El Hierro, Western Canaries. Estud. Geol. 57, 175–273.

Carracedo, J.C., Badiola, R., Guillou, H., 2001. Norte de La Palma. Mapa Geológico Nacional de España (MAGNA). Hojas 1083-I-1083 IV.

Cervelli, P., Segall, P., Johnson, K., Lisowski, M., Mikilius,

A., 2002. Sudden aseismic slip on the south flank of Kilauea volcano. Nature 415, 1014–1018.

Clague, D.A., Denlinger, R.P., 1994. Role of olivine cumulates in destabilizing the flanks of Hawaiian volcanoes. Bull. Volcanol. 56, 425–434.

Day, S.J., Carracedo, J.C., Guillou, H., Gravestock, P., 1999. Recent structural evolution of the Cumbre Vieja volcano, La Palma, Canary Islands: volcanic rift zone reconfiguration as a precursor to volcano flank instability? J. Volcanol. Geotherm. Res. 94, 135–167.

Denlinger, R.P., Okubo, P., 1995. Structure of the mobile south flank of Kilauea Volcano, Hawaii. J. Geophys. Res. 100, 24499–24507.

Delaney, P.T., Miklius, A., Arnadottir, T., Okamura, A.T., Sakao, M.K., 1993. Motion of Kilauea volcano during sustained eruption from the Puu Oo and Kupaianaha vents, 1983-1991. J. Geophys. Res. 98, 17801–17820.

Delaney, P.T., Denlinger, R.P., Lisowski, M., Miklius, A., Okubo, P.G., Okamura, A.T., Sako, M.K., 1998. Volcanic spreading at Kilauea, 1976-1996. J. Geophys. Res. 103, 18003–18023.

Dieterich, J.H., 1988. Growth and persistence of Hawaiian volcanic rift zones. J. Geophys. Res. 93, 4258–4270.

Dvorak, J.J., 1994. An earthquake cycle along the south flank of Kilauea Volcano, Hawaii. J. Geophys. Res. 99, 9533–9541.

Elsworth, D., Voight, B., 1995. Dike intrusion as a trigger for large earthquakes and the failure of volcano flanks. J. Geophys. Res. 100, 6005–6024.

Elsworth, D., Voight, B., 1996. Evaluation of volcano flank instability triggered by dyke intrusion. In: McGuire, W.J., Jones, A.P., Neuberg, J. (Eds.), Volcano Instability on the Earth and Other Planets. Geol. Soc. London 110, 45–53.

Fiske, R.S., Jackson, E.D., 1972. Orientation and growth of Hawaiian volcanic rifts. Proc. R. Soc. London A 329, 299–326.

Gudmundsson, A., Marinoni, L.B., Marti, J., 1999. Injection and arrest of dykes: implications for volcanic hazards. J. Volcanol. Geotherm. Res. 88, 1–13.

Guillou, H., Carracedo, J.C., Duncan, R.A., 2001. K-Ar, 40Ar-39Ar ages and magnetostratigraphy of Brunhes and Matuyama lava sequences from La Palma Island. J. Volcanol. Geotherm. Res. 106, 175–194.

Ida, Y., 1999. Effect of the crustal stress on the growth of dikes: Conditions of intrusion and extrusion of magma. J. Geophys. Res. 104, 17897–17909.

Iverson, R.M., 1995. Can magma-injection and groundwater forces cause massive landslides on Hawaiian volcanoes? J. Volcanol. Geotherm. Res. 66, 295–308.

Komuro, H., Fujita, Y., Kodama, K., 1984. Numerical and experimental models on the formation mechanism of collapse basins during the Green Tuff orogenesis of Japan. Bull. Volcanol. 47, 649–666.

Luongo, G., Cubellis, E., Obrizzo, F., Petrazzuoli, S.M., 1991. A physical model for the origin of volcanism of the Tyrrhenian margin: the case of the Neapolitan area. J. Volcanol. Geotherm. Res. 48, 173–185.

Marti, J., Ablay, G.J., Redshaw, L.T., Sparks, R.S.J., 1994. Experimental studies on caldera collapse. J. Geol. Soc. London 151, 919–929.

McFarlane, D.J., Ridley, W.I., 1968. An interpretation of gravity data for Tenerife, Canary Islands. Earth Planet. Sci. Lett. 4, 481–486.

McGuire, W.J., Pullen, A.D., 1989. Location and orientation of eruptive fissures and feeder-dykes at Mount Etna; influence of gravitational and regional tectonic stress regimes. J. Volcanol. Geotherm. Res. 38, 325–344.

McGuire, W.J., Pullen, A.D., Saunders, S.J., 1990. Recent dyke-induced large-scale block movement at Mount Etna and potential slope failure. Nature 343, 357–359.

Merle, O., Borgia, A., 1996. Scaled experiments of volcanic spreading. J. Geophys. Res. 101, 13805–13817.

Mitchell, N.C., 2001. Transition from circular to stellate forms of submarine volcanoes. J. Geophys. Res. 106, 1987–2003.

Moore, J.G., Clague, D.A., Holcomb, R.T., Lipman, P.W., Normark, W.R., Torresan, M.E., 1989. Prodigious submarine landslides on the Hawaiian Ridge. J. Geophys. Res. 94, 17465–17484.

Nakamura, K., 1980. Why do long rift zones develop in Hawaiian volcanoes; a possible role of thick oceanic sediments. Bull. Geol. Soc. Jpn. 25, 255–269.

Owen, S., Segall, P., Freymueller, J., Miklius, A., Denlinger, R., 1995. Rapid deformation of the south flank of Kilauea volcano. Hawaii. Sci. 267, 1328–1332.

Pollard, D.D., Delaney, P.T., Duffield, W.A., Endo, E.T., Okamura, A.T., Delaney, T., 1983. Surface deformation in volcanic rift zones. In: Morgan, P., Baker, B.H. (Eds.), Processes of Continental Rifting, vol. 94. Elsevier, pp. 541–584.

Richards, R., Jr., Mark, R., 1966. Gelatin models for photoelastic analysis of gravity structures. Exp. Mech. 6, 30–38.

Ryan, M.P., 1988. The mechanics and three-dimensional internal structure of active magmatic systems: Kilauea Volcano, Hawaii. J. Geophys. Res. 93, 4213–4248.

Rubin, A.M., Pollard, D.D., 1987. Origins of blade-like dikes in volcanic rift zones. In: Decker, R.W., Wright, T.L., Stauffer, P.H. (Eds.), Volcanism in Hawaii. U.S. Geol. Surv. Prof. Pap. 1350, 1449–1470.

Staudigel, H., Schmincke, H.-U., 1984. The Pliocene seamount series of La Palma, Canary Islands. J. Geophys. Res. 89, 11195–11215.

Swanson, D.A., Duffield, W.A., Fiske, R.S., 1976. Displacement of the south flank of Kilauea Volcano; the result of forceful intrusion of magma into the rift zones. U.S. Geol. Surv. Prof. Pap. 963, 1–39.

Tilling, R.I., Dvorak, J.J., 1993. Anatomy of a basaltic volcano. Nature 363, 125–133.

Troise, C., 2001. Stress changes associated with volcanic sources: constraints on Kilauea rift dynamics. J. Volcanol. Geotherm. Res. 109, 191–203.

Troll, V.R., Walter, T.R., Schmincke, H.-U., 2002. Cyclic caldera collapse: Piston or piecemeal subsidence? Field and experimental evidence. Geology 30, 135–138.

Vogt, P.R., Smoot, N.C., 1984. The Geisha Guyots: Multibeam bathymetry and morphometric interpretation. J. Geophys. Res. 89, 11085–11107.

Walker, G.P.L., 1987. The dike complex of Koolau Volcano, Oahu; internal structure of a Hawaiian rift zone. In: Decker, R.W., Wright, T.L., Stauffer, P.H. (Eds.), Volcanism in Hawaii. U.S. Geol. Surv., 961–993.

Walker, G.P.L., 1992. Coherent intrusion complexes in large basaltic volcanoes; a new structural model. In: Cox, K.G., Baker, P.E. (Eds.), Essays on Magmas and Other Earth Fluids, vol. 50. Elsevier, pp. 41–54.

Walker, G.P.L., 1999. Volcanic rift zones and their intrusion swarms. J. Volcanol. Geotherm. Res. 94, 21–34.

Walter, T.R., Troll, V.R., 2001. Formation of caldera periphery faults: an experimental study. Bull. Volcanol. 63, 191–203.

Walter, T.R., Schmincke, H.-U., 2002. Rifting, recurrent landsliding and Miocene structural reorganization on NW-Tenerife (Canary Islands). Int. J. Earth Sci. 91, 615–628.

Walter, T.R., 2003. Buttressing and fractional spreading of Tenerife; an experimental approach on the formation of rift zones. Geophys. Res. Lett. 30, 1296.

Watts, A.B., 2001. Isostasy and Flexure of the Lithosphere. Cambridge Univ. Press, 472 pp.

Watters, R.J., Zimbelman, D.R., Bowman, S.D., Crowley, J.K., 2000. Rock mass strength assessment and significance to edifice stability, Mount Rainier and Mount Hood, Cascade Range Volcanoes. Pure Appl. Geophys. 157, 957–976.